Journal of Advanced Research in Fluid Mechanics and Thermal Sciences

Journal homepage:
https://semarakilmu.com.my/journals/index.php/fluid_mechanics_thermal_sciences/index
ISSN: 2289-7879

Numerical Investigation of Diffusion Thermo and Thermal Diffusion on MHD Convective Flow of Williamson Nanofluid on a Stretching Surface Through a Porous Medium in the Presence Chemical Reaction and Thermal Radiation

Bavanasi Pradeep Kumar[1,*], Sangapatnam Suneetha[2]

[1] Department of Applied Mathematics, Yogi Vemana University, Kadapa district, Andhra Pradesh 516005, India

ARTICLE INFO

Article history:
Received 18 October 2023
Received in revised form 1 March 2024
Accepted 10 March 2024
Available online 30 March 2024

Keywords:
Williamson nanofluid; MHD; diffusion thermo; thermal diffusion; thermal radiation

ABSTRACT

In this paper, analyze the impact of Diffusion thermo and thermal diffusion with heat and mass transfer inherent of thermally radiant Williamson nanofluid over a stretyching surface through a porous medium under the convective boundary condition in the presence of thermal radiation and chemical reaction has been studied. The coefficients of Brownian and thermophoresis diffusions are also taken into consideration. The governing partial differential equations are reduced to a couple of nonlinear ordinary differential equations by using suitable transformation equations; these equations are then solved numerically with the use of the conventional fourth-order Runge Kutta method accompanied by the shooting technique. As a result, the effects of various physical parameters on the velocity, temperature, and nanoparticle concentration profiles as well as on the skin friction coefficient and rate of heat transfer are discussed with the aid of graphs and tables. This study has been directly applied in the pharmaceutical industry, microfluidic technology, microbial improved oil recovery, modelling oil and gas-bearing sedimentary basins, and many other fields. Further, to check the accuracy and validation of the present results, satisfactory concurrence is observed with the existing literature.

1. Introduction

Non-Newtonian fluids are extensively implemented in diverse industrial processes such as petroleum drilling, drawing of plastic films, fibre spinning, and food production. The Williamson fluid model is one of the simplest non-Newtonian models to replicate the viscoelastic shear-thinning attributes, see Williamson [1]. The flow of thermally radiative Williamson fluid on a stretching sheet with chemical reaction was disclosed by Krishnamurthy *et al.,* [2]. They proved the fluid temperature falling off due to the presence of the Williamson parameter. Khan *et al.,* [3] demonstrated the impact of slip flow of Williamson nanofluid in a porous medium. They exposed that the surface drag force

* *Corresponding author.*
E-mail address: myresearch2026@gmail.com

https://doi.org/10.37934/arfmts.115.2.141157

suppresses due to rising the Williamson fluid parameter. The 2D unsteady radiative Williamson fluid flow on a permeable stretching surface was deliberated by Hayat *et al.,* [4]. They noticed that the fluid speed becomes slow when the Williamson parameter is high. Nadeem *et al.,* [5] examined the Williamson fluid flow past a stretching sheet, and they found that the skin friction coefficient decreases with enhancing the Williamson parameter. Make use of the Keller box procedure to solve the problem of MHD flow of Williamson fluid over a stretching sheet by Salahuddin *et al.,* [6]. Their outcome shows that the Williamson fluid parameter leads to suppress the fluid velocity. Few significant analysis for this area is seen in a study by Khan and Khan [7].

Heat and mass transfer in non-Newtonian fluid flow through porous medium in engineering has extensive application, such as ventilation procedure, oil production, solar collection, cooling of nuclear reactors, and electronic cooling. Accordingly, Maripala and Kishan [8] investigated the effect of thermal radiation and chemical reaction on time-dependent MHD flow and heat transfer of nanofluid over a permeable shrinking sheet. Their result indicates that with an increase of the suction parameter, the temperature profiles decrease whereas the concentration profiles upsurge. Moreover, RamReddy and Kairi [9], Lakshmi *et al.,* [10], Ambreen *et al.,* [11], Aurangzaib *et al.,* [12], Reddy *et al.,* [13], Al-Mamun *et al.,* [14], and Ahmed *et al.,* [15] studied mixed convective heat and mass transfer of MHD nanofluids embedded in porous medium over stretching surfaces. From their result, it can be seen that temperature distribution and thermal boundary layer reduce with an increase of dimensionless thermal free convection parameter, dimensionless mass free convection parameter, and Prandtl number.

When heat and mass transfer occur simultaneously in a moving fluid, the energy flux caused by a concentration gradient is termed as diffusion thermo effect, whereas mass fluxes can also be created by temperature gradients which is known as a thermal diffusion effect. These effects are studied as second-order phenomena and may have significant applications in areas like petrology, hydrology, and geosciences. The effect of thermophoresis on an unsteady natural convection flow and heat and mass transfer of micropolar fluid with Soret and Dufour effects was studied by Aurangzaib *et al.,* [16]. Srinivasacharya and RamReddy [17] considered the problem of the steady MHD mixed convection heat and mass transfer of micropolar fluid through non-Darcy porous medium over a semi-infinite vertical plate with Soret and Dufour effects. Influence of the Soret and Dufour numbers on mixed convection flow and heat and mass transfer of non-Newtonian fluid in a porous medium over a vertical plate was analyzed by Mahdy [18]. Hayat and Nawaz [19] investigated analytically the effects of the Hall and ion slip on the mixed convection heat and mass transfer of second-grade fluid with Soret and Dufour effects. Rani and Kim [20] studied numerically the laminar flow of an incompressible viscous fluid past an isothermal vertical cylinder with Soret and Dufour effects. The effects of chemical reaction and Soret and Dufour on the mixed convection heat and mass transfer of viscous fluid over a stretching surface in the presence of thermal radiation were analyzed by Pal and Mondal [21]. Sharma *et al.,* [22] studied the mixed convective flow, heat and mass transfer of viscous fluid in a porous medium past a radiative vertical plate with chemical reaction, and Soret and Dufour effects.

Activation energy is the smallest amount of energy needed by chemical reactants to endure a chemical reaction. The influence of activation energy on convective heat and mass transfer in the region of boundary layers was initially inspected by Bestman [23]. Later, many researchers have studied the impact of activation energy on heat and mass transfer of boundary layer flow of the fluids. Among those researchers, Awad *et al.,* [24], Dhlamini *et al.,* [25], Anuradha and Sasikala [26], and Hamid and Khan [27] scrutinized the influence of activation energy on heat and mass transfer in unsteady fluid flow under different geometry. Moreover, Huang [28] and Mustafa *et al.,* [29] studied the effect of activation energy on MHD boundary layer flow of nanofluids past a vertical surface and permeable horizontal cylinder. Further investigations on the effect of activation energy on non-

Newtonian fluid under different surfaces are stated in previous studies [30-32]. Bouslimi *et al.,* [33] have studied MHD Williamson Nanofluid Flow over a Stretching Sheet through a Porous Medium under Effects of Joule Heating, Nonlinear Thermal Radiation, Heat Generation/Absorption, and Chemical Reaction. From their plots, it can be seen that as the values of the activation energy parameter upsurges, the concentration nanoparticles increase.

The aforementioned studies and open literature survey bear witness effects of Diffusion thermo and Thermal Diffusion on two-dimensional laminar and incompressible steady flow of thermally radiant Williamson nanofluid through vertical cone with porous material in the presence of thermal radiation has been presented. The highly non-linear partial differential equations are simplified by using suitable similarity transformation equations and the reduced equations are solved numerically with the help of the conventional fourth-order Runge-Kutta method along with the shooting procedure. Discussion on the results is deliberated through graphs and tables for some pertinent parameters of interest. Moreover, a comparison of the numerical results was checked and the validity of the method with published works was made; it shows nice agreement.

2. Flow Governing Equations

In the beginning, the study of Williamson nanofluid flow can be shown in several steps

i. The first step is the fluid flow being steady and incompressible,
ii. The second step is that the flowing process is two-dimensional flow on a stretching surface through a porous medium and,
iii. The third step is the plate is stretched along the x-axis with a velocity $U_w(x) = Bx$, where B is the stretching rate.

The coordinate's x, y are in the flow direction and normal to the flow direction, respectively. The applied magnetic field, heat generation, and viscous dissipation effects are encountered. The schematic diagram of flow is given in Figure 1. By following Bouslimi *et al.,* [33], the governing equations are given below:

$$\frac{\partial u}{\partial x}+\frac{\partial v}{\partial y}=0 \tag{1}$$

$$u\frac{\partial u}{\partial x}+v\frac{\partial u}{\partial y}=\upsilon\frac{\partial^2 u}{\partial x^2}-\sqrt{2}\upsilon\Gamma\frac{\partial u}{\partial y}\frac{\partial^2 u}{\partial y^2}-\frac{\sigma B_0^2}{\rho}u-\frac{\vartheta}{k}u, \tag{2}$$

$$u\frac{\partial T}{\partial x}+v\frac{\partial T}{\partial y}=\alpha\frac{\partial^2 T}{\partial y^2}+\tau\left(D_B\left(\frac{\partial T}{\partial y}\frac{\partial C}{\partial y}\right)+\frac{D_T}{T_\infty}\left(\frac{\partial T}{\partial y}\right)^2\right)-\frac{1}{\left(\rho C_p\right)_f}\frac{\partial q_r}{\partial y}+\frac{\sigma B_0^2}{\left(\rho C_p\right)_f}u^2+\frac{Q}{\left(\rho C_p\right)_f}\left(T-T_\infty\right)+\frac{D_m k_T}{c_s c_p}\frac{\partial^2 C}{\partial y^2} \tag{3}$$

$$u\frac{\partial C}{\partial x}+v\frac{\partial C}{\partial y}=\frac{D_m k_T}{T_m}\frac{\partial T^2}{\partial y^2}+D_B\frac{\partial^2 C}{\partial y^2}+\left(\frac{D_T}{T_\infty}\right)\frac{\partial T^2}{\partial y^2}-R^*\left(C-C_\infty\right) \tag{4}$$

For this flow, corresponding boundary conditions are

$$\begin{aligned} &u = U_w,\ v = 0,\quad T = T_w,\quad D_B\frac{\partial C}{\partial y} + \frac{D_T}{T_\infty}\frac{\partial T}{\partial y} = 0 \qquad at\ \ y = 0 \\ &u \to 0,\quad v \to 0,\quad T \to T_\infty,\quad C \to C_\infty \qquad as\ y \to \infty \end{aligned} \tag{5}$$

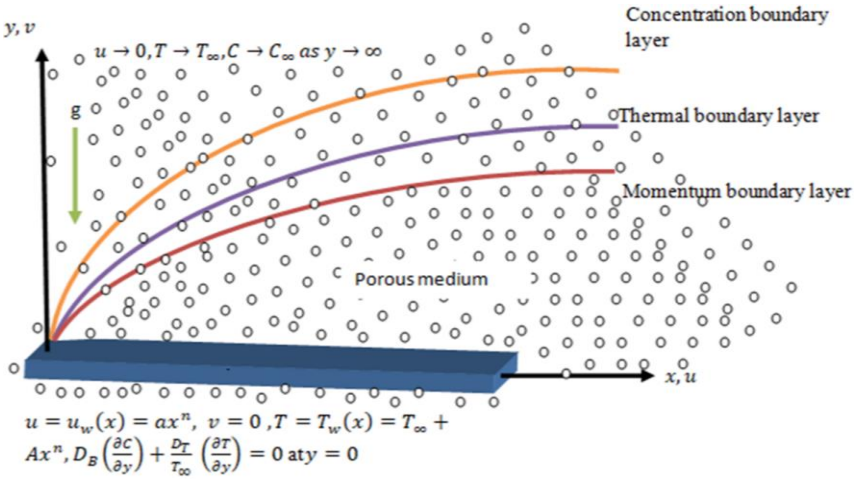

Fig. 1. Flow configuration

where u is the velocity components in the direction of the x -axis and v is the velocity components in the direction of the y-axis; in addition, α represent the thermal diffusivity, ρ refer to density of the fluid, and v is the kinematic viscosity of fluid; also, T and T_∞, respectively, are fluid temperature and ambient fluid temperature. A uniform magnetic field of strength B_0 is applied in the transverse direction of the flow; due to the small magnetic Reynolds number, it is not necessary to introduce the effect of the induced magnetic field. It should be noted that D_B, D_T, σ, c_P, and R^* are, respectively, the Brownian diffusion coefficient, the thermophoresis diffusion coefficient, the electrical conductivity, the specific heat at constant pressure, and destructive and constructive reaction rates. Here, C and C_∞ are the concentration of nanoparticles and ambient nanoparticle concentration. It is worth noting that the effect of nonlinear thermal radiation, heat source/- sink, and Joule heating is taken in the energy equation. The viscous dissipation is assumed to be negligibly small in the energy equation. The effects of the homogenous chemical reaction are taken in the concentration equation.

The radiative heat flux q_r (using Roseland approximation followed Awad *et al.,* [24]) is defined as

$$q_r = -\frac{4\sigma^*}{3K^*}\left(\frac{\partial T^4}{\partial y}\right) \tag{6}$$

We assume that the temperature variances inside the flow are such that the term T^4 can be represented as linear function of temperature. This is accomplished by expanding T^4 in a Taylor series about a free stream temperature T_∞ as follows

$$T^4 = T_\infty^4 + 4T_\infty^3\left(T - T_\infty\right) + 6T_\infty^2\left(T - T_\infty\right)^2 + \ldots\ldots\ldots \tag{7}$$

After neglecting higher-order terms in the above equation beyond the first degree term in $\left(T-T_{\infty}\right)$, we get

$$T^4 \cong 4T_{\infty}^3 T - 3T_{\infty}^4 \tag{8}$$

Thus substituting Eq. (8) in Eq. (6), we get

$$q_r = -\frac{16T_{\infty}^3\sigma^*}{3K^*}\left(\frac{\partial T}{\partial y}\right) \tag{9}$$

Using (9), Eq. (3) can be written as

$$u\frac{\partial T}{\partial x}+v\frac{\partial T}{\partial y}=\alpha\frac{\partial^2 T}{\partial y^2}+\frac{1}{\left(\rho C_p\right)_f}\frac{16\sigma^*}{3K^*}\frac{\partial}{\partial y}\left(T_{\infty}^3\frac{\partial T}{\partial y}\right)+\frac{\left(\rho C_p\right)_p}{\left(\rho C_p\right)_f}\left(D_B\left(\frac{\partial T}{\partial y}\frac{\partial C}{\partial y}\right)+\frac{D_T}{T_{\infty}}\left(\frac{\partial T}{\partial y}\right)^2\right)+ \frac{\sigma B_0^2}{\left(\rho C_p\right)_f}u^2+\frac{Q}{\left(\rho C_p\right)_f}\left(T-T_{\infty}\right)+\frac{D_m k_T}{c_s c_p}\frac{\partial^2 C}{\partial y^2} \tag{10}$$

where σ* and k* are the Stefan-Boltzmann constant and mean absorption coefficient. The similarity transformations and non-dimensional variables can be written as follows

$$\eta=\sqrt{\frac{U_w(x)}{vx}}y, u=Bxf'(\eta), v=-\sqrt{Bx}\,f(\eta),\ \theta(\eta)=\frac{T-T_{\infty}}{T_w-T_{\infty}},\ \phi(\eta)=\frac{C-C_{\infty}}{C_w-C_{\infty}} \tag{11}$$

where η is the similarity variable and f(η), θ(η), and ϕ(η), respectively, are the dimensionless stream function, temperature, and concentration of nanoparticles; the similarity transformations and the nondimensional variables (6) were used to convert the boundary layer governing partial differential Eq. (2), Eq. (3), and Eq. (4) to a set of ordinary differential equations taking the mathematical formulas

$$f'''(\eta)+Wf''(\eta)f'''(\eta)-Mf'(\eta)-f'(\eta)^2+f(\eta)f''(\eta)-Daf'(\eta)=0 \tag{12}$$

$$\theta''(\eta)(1+R_d)+\Pr\left[\begin{array}{l}\left(N_b\,\theta'(\eta)\phi'(\eta)+N_t(\theta'(\eta))^2\right)+Q_0\theta(\eta)+\\ ME_c(f'(\eta))^2+\theta'(\eta)f(\eta)+D_u\,\phi'\end{array}\right]=0 \tag{13}$$

$$\phi''(\eta)+L_e\left[f(\eta)\phi'(\eta)-R_c\phi(\eta)+S_r\theta''(\eta)\right]+\left(\frac{N_t}{N_b}\right)\theta''(\eta)=0 \tag{14}$$

The corresponding boundary conditions (5) become

$$\begin{array}{l}f(0)=0,\quad f'(0)=1,,\theta'(0)=1,N_b\phi'(0)+Nt\theta'(0)=0\\ f'(\infty)\to 0,\ \theta(\infty)\to 0,\ \phi(\infty)\to 0.\end{array} \tag{15}$$

where prime denotes differentiation with respect to η, and the significant thermo physical parameters indicating the flow dynamics are defined by

$M = \frac{\sigma B_0^2}{\rho B}$ is the magnetic field parameter, $W = \Gamma x\sqrt{\frac{2B^3}{\nu}}$ is the non-Newtonian williamson parameter, $\Pr = \frac{\nu}{\alpha}$ is the Prandtl number, $N_b = \frac{(\rho C_p)_p}{(\rho C_p)_f}\frac{D_B(C_w - C_\infty)}{\nu}$ is the Brownian motion parameter, $N_t = \frac{(\rho C_p)_p}{(\rho C_p)_f}\frac{D_T(T_w - T_\infty)}{\upsilon T_\infty}$ is the thermophoresis parameter, $L_e = \frac{\nu}{D_B}$ is the Lewis number, $D_a = \frac{\mu}{\rho BK}$ is the Darcy number, $Q_0 = \frac{Q}{B(\rho C_p)_f}$ is the heat generation (Q_0>0) or absorption (Q_0<0) parameter, $R_c = \frac{R^*}{B}$ is the chemical reaction parameter, $Ec = \frac{U_w^2(x)}{C_p(T_w - T_\infty)}$ is the non-dimensional activation energy, $R_d = \frac{16\sigma^* T_\infty^3}{3kK^*}$ is the thermal Radiation parameter, $Du = \frac{D_M k_T(C_w - C_\infty)}{C_S C_p \upsilon \alpha^2 (T_w - T_\infty)}$ is the Diffusion thermo parameter, $S_r = \frac{D_m k_T(T_w - T_\infty)}{T_m \alpha_m (C_w - C_\infty)}$ is the Thermal Diffusion parameter.

The quantities we are interested to study are the skin friction coefficient C_f, the local Nusselt number N_{ux} and the local Sherwood number S_{hx}. The quantities are defined as:

$$C_f = \frac{\tau_w}{\rho u_w^2} = \frac{\mu\left[\frac{\partial u}{\partial y} + \frac{\Gamma}{\sqrt{2}}\left(\frac{\partial u}{\partial y}\right)^2\right]_{y=0}}{\rho\left(\frac{x\upsilon}{L^2}\right)} = f''(0) + \frac{W}{2}f''^2(0) \tag{16}$$

$$Nu_x = \frac{xq_w}{k(T_w - T_\infty)} = \frac{-x\left(\frac{\partial T}{\partial y}\right)_{y=0}}{k(T_w - T_\infty)} = -\theta'(0), \tag{17}$$

$$Sh_x = \frac{x\, j_w}{D_B(C_w - C_\infty)} = \frac{-x\left(\frac{\partial C}{\partial y}\right)_{y=o}}{D_B(C_w - C_\infty)} = -\phi'(0). \tag{18}$$

3. Numerical Solution

As Eq. (12) - (14) are strongly non-linear, it is difficult or maybe impossible to find the closed form solutions. Accordingly, these boundary value problems are solved numerically by using the conventional fourth-order RK integration scheme along with the shooting technique. The first task to carry out the computation is to convert the boundary value problem to an initial value problem.

The first task to carry out the computation is to convert the boundary value problem to an initial value problem.

Let by using the following notations

$$f = y_1,\ f' = y_2, f'' = y_3,\ f''' = y_3',\quad \theta = y_4,\ \theta' = y_5, \theta'' = y_5',\ \phi = y_6,\ \phi' = y_7, \phi'' = y_7'. \tag{19}$$

By using the above variables, the system of first-order ODEs is

$$y_1' = y_2, \tag{20}$$

$$y_2' = y_3, \tag{21}$$

$$y_3' = \frac{1}{1 + y_3 W}\left(M y_2 + y_2^2 - y_1 y_3 + Da\, y_2\right), \tag{22}$$

$$y_4' = y_5, \tag{23}$$

$$y_5' = \frac{-\Pr}{1 + R_d}\left(N_b y_5 y_7 + Nt(y_5)^2 + Q_0 y_5 + ME_c(y_2)^2 + y_5 y_1 + Du\, y_7\ \right), \tag{24}$$

$$y_6' = y_7, \tag{25}$$

$$y_7' = -L_e\left[y_1 y_7 - R_c y_7 + S_r L_e y_5'\right] - \left(\frac{N_b}{N_t}\right)(y_7')^2 \tag{26}$$

4. Code Validation

To ensure the accuracy and correctness of the numerical solutions of the current study, a numerical comparison was made between the numerical values and results of the current study with the numerical values and results of the work published by Bouslimi *et al.,* [33] in Table 1. The great convergence between the two studies was noted, which gives high credibility to the current study.

Table 1
A comparison between the numerical results of Bouslimi *et al.,* [33] and the results of the current study through the values of in the case of as When, Du=Sr=0

Nt	Nb=0.1		Nb=0.2		Nb=0.2	
	Bouslimi *et al.,* [33]	Present Study	Bouslimi *et al.,* [33]	Present Study	Bouslimi *et al.,* [33]	Present Study
0.1`	0.9501	0.9553	0.5065	0.5075	0.2534	0.2565
0.2	0.6910	0.69856	0.3646	0.3686	0.1912	0.1945
0.3	0.5237	0.5867	0.2735	0.2786	0.1382	0.1376
0.4	0.4083	0.4009	0.2124	0.2168	0.1086	0.1051
0.5	0.4083	0.4005	0.1710	0.17875	0.0880	0.0732

5. Results and Discussion

After converting the system of partial differential equations ruling to study the flow of fluid into a system of ordinary differential equations, it has a set of important parameters that we list in the following order M, Da and "W" which are the magnetic field, the Darcy number, and non-Newtonian Williamson parameters, respectively, while Rd and Q_0 represent the nonlinear thermal radiation, and the heat generation/absorption parameters, respectively; also, Pr is the Prandtl number and Nt is the thermophoresis parameter, while , Ec, Rc, Le and Nb are the Eckert number, the chemical reaction, the Lewis number, and Brownian motion parameters, respectively. The effect of all the previous physical parameters on the velocity, temperature, and concentration of nanoparticle distributions has been studied by making graphical figures that clarify this and by showing the physical meanings of each parameter and its importance in this study, and we can list the results of this study in detail.

The set of nonlinear equations with appropriate boundary conditions are solved numerically by Runge Kutta method along with the shooting procedure. To analyze the variation in velocity, thermal, and concentration distributions, Figure 3 to Figure 7 are displayed. Also, the skin friction factor, Nusselt number, and Sherwood number are displayed through Table 2. For the present analysis, the values of fixed parameters are taken as Le=2, Pr=5, Rc=0.6, Rd=1.2, Nb 0.5, Nt=0.5, Da=0.5, Ec=0.4, W=0.2, Du=0.5, Sr=0.5 and M = 0.5.

Figure 2 to Figure 4 show the impact of the Williamson parameter on velocity, temperature, and concentration distributions. Here, the reducing impact on velocity distribution is perceived with a higher Williamson parameter, while a reducing impression on thermal and concentration distributions is depicted for both geometries. Physically, the increasing Williamson parameter suggests more retardation time for the nanofluid flow particles to regain their original position, increasing the fluid viscosity and, consequently, reducing the velocity distribution. Also, the greater values of the Williamson factor provide more resistance to the nanofluid flow, which concludes enhancement in thermal and concentration of the nanofluid flow.

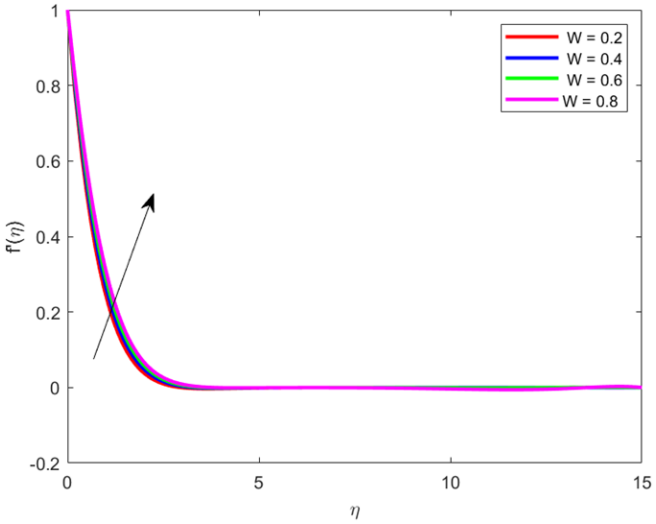

Fig. 2. Effect of W on velocity profile

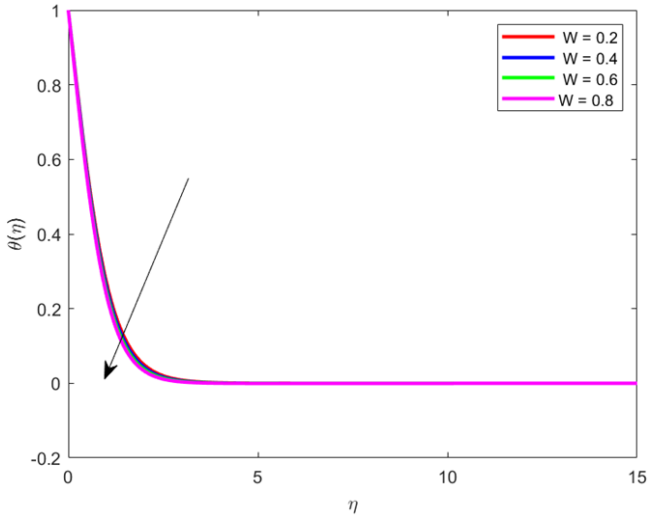

Fig. 3. Effect of W on temperature profile

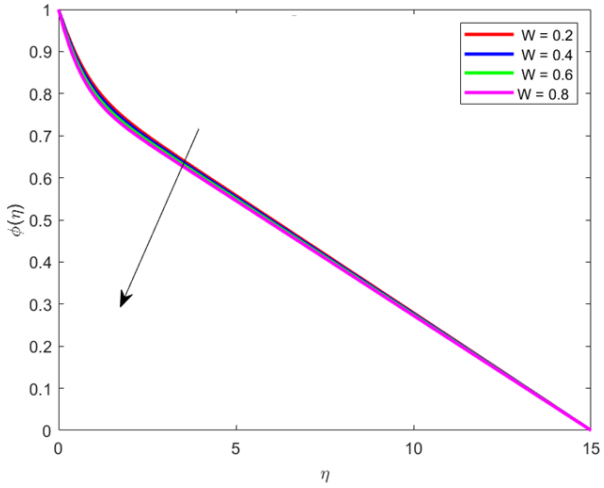

Fig. 4. Effect of W on concentration profile

Figure 5 and 6 show the effect of the strength of the magnetic field parameter on the fluid velocity and temperature distribution. It is noticeable that the result of this effect is negative in the sense that the relationship between the magnetic field and the velocity distribution is inverse; the increase in the values of the magnetic field means a decrease in the velocity of the fluid. Physically, when influencing a moving fluid by the magnetic field, the fluid particles are stimulated, which creates a kind of counter force that slows and reduces the fluid's motion; moreover, this force is perpendicular to the velocity vector on the one hand and also perpendicular to the magnetic field vector on the other hand which is originally a resistance force called Lorentz force, while highlighting that the increase in the magnetic field reduces the thickness of the boundary layer. The reverse trend has observed in the case of temperature as shown in Figure 6.

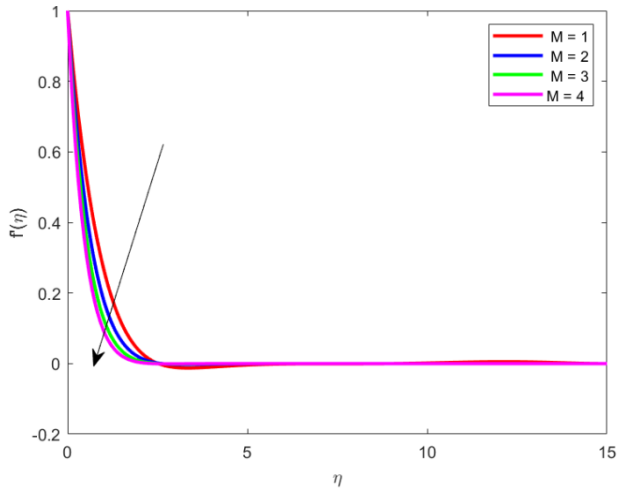

Fig. 5. Effect of M on velocity profile

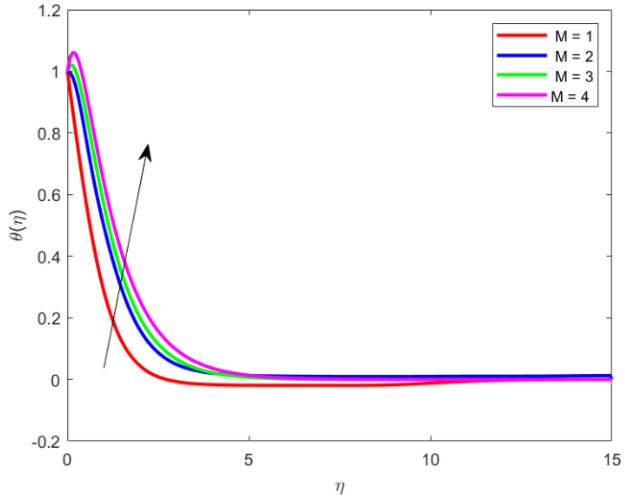

Fig. 6. Effect of W on temperature profile

The temperature and concentration profiles for different values of Brownian motion parameter (Nb) is summarized in Figure 7 and 8. It is investigated that an increases in (Nb), the temperature is extends as shown in Figure 7, whereas the concentration profiles depreciate in Figure 8. This is because of the Brownian motion is the random motion of suspended nanoparticles in the base fluid and is more influenced by its fast moving atoms or molecules in the base fluid. It is mentioned that Brownian motion is related to the size of nanoparticles and are often in the form of agglomerates. Clearly, it can be concluded that Brownian motion parameter has significant influence on the both temperature and concentration.

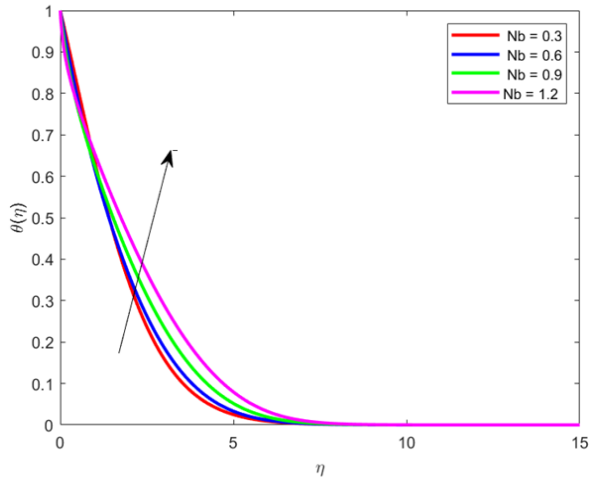

Fig. 7. Effect of Nb on temperature profile

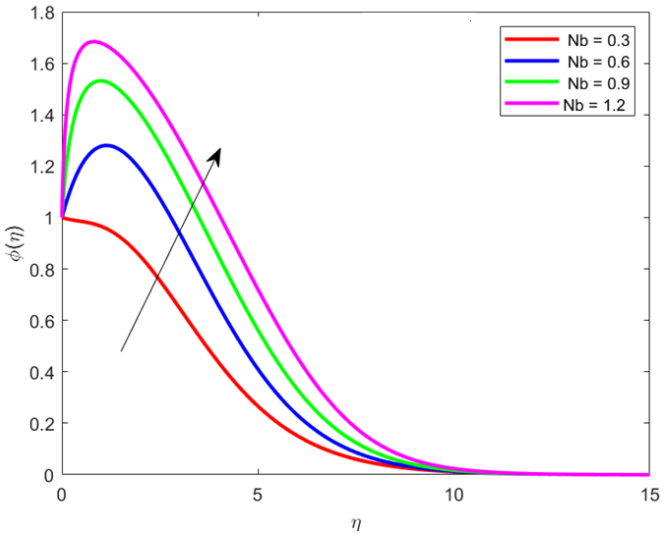

Fig. 8. Effect of Nb on concentration profile

The Variation of non-dimensional temperature and concentration distributions for different values of thermophoretic parameter (Nt) is depicted in Figure 9 and 10. It is noticed from these Figure 9 and 10 that both temperature and concentration profiles boosted in the boundary layer region for the accrual values of thermophoretic parameter (Nt). This is because of the fact that as the values of (Nt) increases the hydrodynamic boundary layer thickness is reduced. This is from the reality that particles near the hot surface create thermophoretic force; this force enhances the temperature and concentration of the fluid in the fluid region.

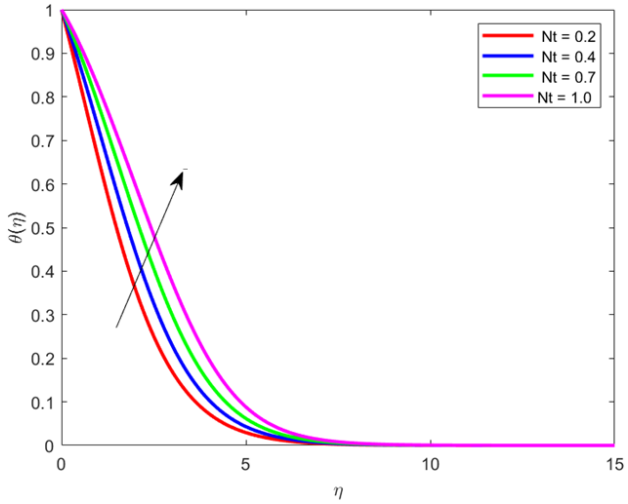

Fig. 9. Effect of Nt on temperature profile

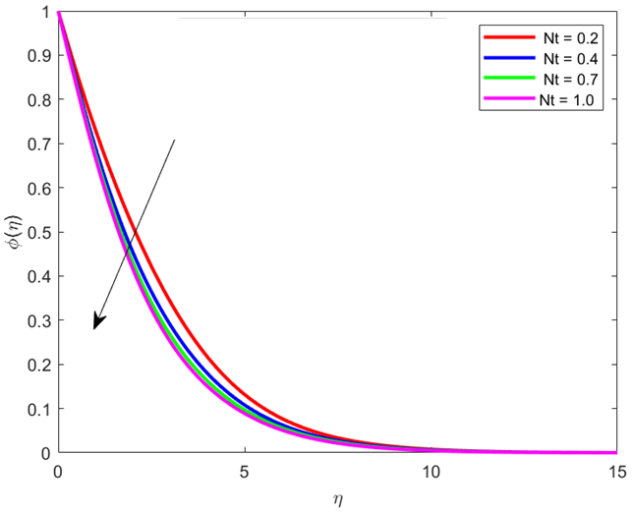

Fig. 10. Effect of Nt on concentration profile

Figure 11 depicts the temperature for the contribution of Diffusion thermo parameter Du. Temperature enhancement is noticed for higher Du values. The effect of thermal radiation parameter (Rd) on temperature profile is shown in Figure 12. It is acknowledged that, the thermal boundary layer thickness is enlarged with improving values of radiation parameter (Rd) in the entire boundary layer region of fluid. This is due to the fact that imposing thermal radiation into the flow warmer the fluid, which causes an increment in the temperature.

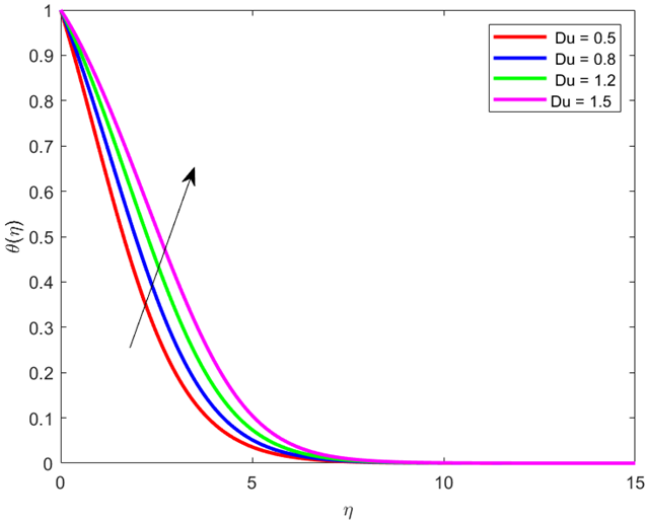

Fig. 11. Effect of Du on temperature profile

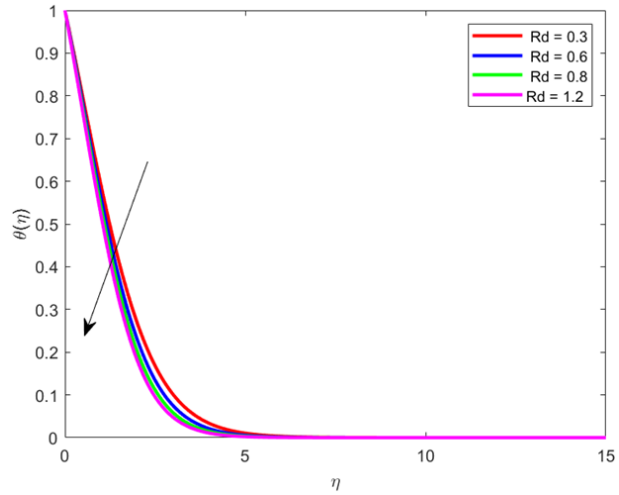

Fig. 12. Effect of Rd on temperature profile

Figure 13 shows the effect of the concentration profiles for different values of Sr. As seen from this graph that concentration of species increases with increasing values of the Soret number leading to an increase in thermal boundary value thickness. It is observed from Figure 14 that increasing the value of chemical reaction parameter Rc decreases the concentration of species in the boundary layer and hence the solutal boundary layer thickness becomes thinner.

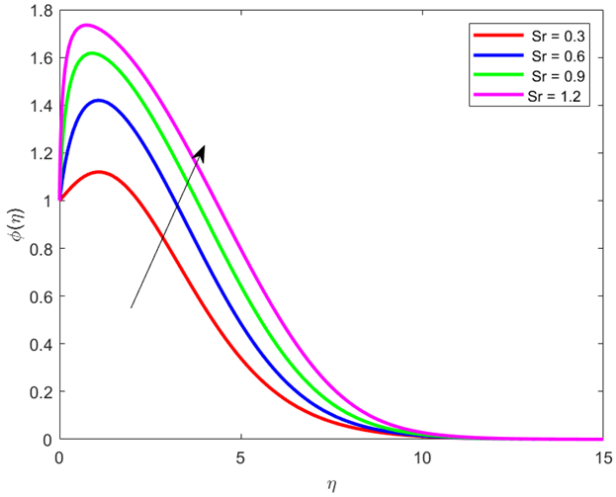

Fig. 13. Effect of Sr on concentration profile

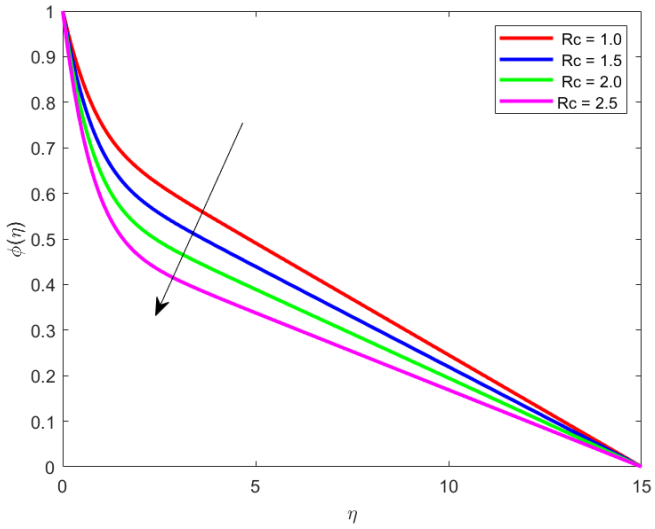

Fig. 14. Effect of Rc on concentration profile

Table 2 shows the numerical values of the local Nusselt number $Nu_x / \sqrt{\mathrm{Re}_x}$ and skin friction coefficient $\sqrt{\mathrm{Re}_x} C_f$ for all physical parameters resulting from the current numerical study of the Williamson fluid flow process that contains nanoparticles on an expanding surface in the presence of a porous medium. The following was observed that the skin friction coefficient $\sqrt{\mathrm{Re}_x} C_f$ has become a constant value for all physical parameters with the exception of each of the magnetic field parameter M, Darcy number Da, and non-Newtonian Williamson parameter λ, whereas the values of the local Nusselt number $Nu_x / \sqrt{\mathrm{Re}_x}$ decrease under the influence of all physical parameters.

Table 2

The numerical values of the skin friction coefficient $\sqrt{\mathrm{Re}_x}C_f$ and the local Nusselt number $Nu_x/\sqrt{\mathrm{Re}_x}$ p for values of M, Da, Du, Sr, Rd and W parameters when Le=2, Pr=5, Rc=0.6, Nb=0.5, Nt=0.5, Ec=0.4

M	Rd	Da	Du	W	Sr	$\sqrt{\mathrm{Re}_x}C_f$	$Nu_x/\sqrt{\mathrm{Re}_x}$
0	1.2	0.5	0.5	0.2	0.5	1.16630705	0.32673441
1						-1.33621158	0.32351790
2						-1.48295534	0.32112657
3						-1.61309297	0.31923008
4						-1.73049604	0.31766292
		1.0				-1.16630705	0.32463205
		1.5				-1.33621158	0.32351790
		2.0				-1.48295534	0.32272607
		2.5				-1.61309297	0.32212446
				0.2		-1.37751997	0.32368673
				0.4		-1.28773536	0.32332326
				0.6		-1.163126387	0.32263272
				0.8		-0.36239912	0.32190223
			0.5			-0.3674850	0.6524254
			0.8			-0.12536745	0.56287266
			1.2			-0.9846584	0.46272794
			1.5			-0.8756375	0.2564782
					0.3	-0.98464656	0.3846402
					0.6	-0.1625257	0.3888543
					0.9	-0.1967435	0.3908264
					1.2	-0.3254265	0.39996355
	0.3					-0.3784757	0.4363766
	0.6					-0.2904986	0.3637376
	0.8					-0.1537386	0.3084376
	1.2					-0.0383635	0.29746476

6. Conclusion

The following is a condensed version of the conclusions that may be drawn from the numerical results

i. The velocity distribution of the fluid is negatively affected by the influence of the magnetic field parameter M, and the non-Newtonian Williamson parameter W at the time when their influence on the distributions of the temperature and concentration of the nanoparticles becomes positive.
ii. An increase in thermal radiation parameter results in an increase in temperature field.
iii. With increasing values of (Nb) temperature profiles optimized, whereas, concentration profiles decline in the entire fluid regime.
iv. Both resultant temperature and concentration profiles are enhancing with increases Du and Sr values.

References

[1] Williamson, R. Vo. "The flow of pseudoplastic materials." *Industrial & Engineering Chemistry* 21, no. 11 (1929): 1108-1111. https://doi.org/10.1021/ie50239a035

[2] Krishnamurthy, M. R., B. C. Prasannakumara, B. J. Gireesha, and Rama Subba Reddy Gorla. "Effect of chemical reaction on MHD boundary layer flow and melting heat transfer of Williamson nanofluid in porous medium." *Engineering Science and Technology, an International Journal* 19, no. 1 (2016): 53-61. https://doi.org/10.1016/j.jestch.2015.06.010

[3] Khan, M. Ijaz, Faris Alzahrani, Aatef Hobiny, and Zulfiqar Ali. "Modeling of Cattaneo-Christov double diffusions (CCDD) in Williamson nanomaterial slip flow subject to porous medium." *Journal of Materials Research and Technology* 9, no. 3 (2020): 6172-6177. https://doi.org/10.1016/j.jmrt.2020.04.019

[4] Hayat, T., Anum Shafiq, and A. Alsaedi. "Hydromagnetic boundary layer flow of Williamson fluid in the presence of thermal radiation and Ohmic dissipation." *Alexandria Engineering Journal* 55, no. 3 (2016): 2229-2240. https://doi.org/10.1016/j.aej.2016.06.004

[5] Nadeem, S., S. T. Hussain, and Changhoon Lee. "Flow of a Williamson fluid over a stretching sheet." *Brazilian Journal of Chemical Engineering* 30 (2013): 619-625. https://doi.org/10.1590/S0104-66322013000300019

[6] Salahuddin, T., Md Yousaf Malik, Arif Hussain, S. Bilal, and M. Awais. "MHD flow of Cattanneo-Christov heat flux model for Williamson fluid over a stretching sheet with variable thickness: Using numerical approach." *Journal of Magnetism and Magnetic Materials* 401 (2016): 991-997. https://doi.org/10.1016/j.jmmm.2015.11.022

[7] Khan, Najeeb Alam, and Hassam Khan. "A boundary layer flows of non-Newtonian Williamson fluid." *Nonlinear Engineering* 3, no. 2 (2014): 107-115. https://doi.org/10.1515/nleng-2014-0002

[8] Maripala, Srinivas, and N. Kishan. "Unsteady MHD flow and heat transfer of nanofluid over a permeable shrinking sheet with thermal radiation and chemical reaction." *American Journal of Engineering Research* 4, no. 6 (2015): 68-79.

[9] RamReddy, Ch, and R. R. Kairi. "The effect of melting on mixed convection heat and mass transfer in non-Newtonian nanofluid SATURATEED in porous medium." *Frontiers in Heat and Mass Transfer (FHMT)* 6, no. 1 (2015). https://doi.org/10.5098/hmt.6.6

[10] Lakshmi, G. Vijaya, L. Anand Babu, and K. Srinivasa Rao. "MHD mixed convection stagnation point flow of nanofluid through a porous medium over stretching sheet." *International Journal of Pure and Applied Mathematics* 118, no. 10 (2018): 369-389.

[11] Ambreen, N., A. Rehman, N. Sheikh, S. Iqbal, and M. Zulfiqar. "Boundary-layer flow and heat transfer over a rotating porous disk in a non-Newtonian Williamson nanofluid." *Indian Journal of Science and Technology* 12, no. 38 (2019): 1-38. https://doi.org/10.17485/ijst/2019/v12i38/146120

[12] Aurangzaib, Aurangzaib, A. R. M. Kasim, N. F. Mohammad, and Sharidan Shafie. "Unsteady MHD mixed convection flow with heat and mass transfer over a vertical plate in a micropolar fluid-saturated porous medium." *Journal of Applied Science and Engineering* 16, no. 2 (2013): 141-150.

[13] Reddy, G. Bal, B. Shankar Goud, and M. R. Shekar. "Numerical solution of MHD mixed convective boundary layer flow of a nanofluid through a porous medium due to an exponentially stretching sheet with magnetic field effect." *International Journal of Applied Engineering Research* 14, no. 9 (2019): 2074-2083.

[14] Al-Mamun, Abdullah, S. M. Arifuzzaman, Sk Reza-E-Rabbi, Pronab Biswas, and Md Shakhaoath Khan. "Computational modelling on MHD radiative Sisko nanofluids flow through a nonlinearly stretching sheet." *International Journal of Heat and Technology* 37, no. 1 (2019): 285-295. https://doi.org/10.18280/ijht.370134

[15] Ahmed, Sameh E., Ramadan A. Mohamed, M. Aly Abd Elraheem, and Mahmoud S. Soliman. "Magnetohydrodynamic Maxwell nanofluids flow over a stretching surface through a porous medium: effects of non-linear thermal radiation, convective boundary conditions and heat generation/absorption." *International Journal of Aerospace and Mechanical Engineering* 13, no. 6 (2019): 436-443.

[16] Aurangzaib, A. R. M. K., N. F. Mohammad, and Sharidan Shafie. "Soret and dufour effects on unsteady MHD flow of a micropolar fluid in the presence of thermophoresis deposition particle." *World Applied Sciences Journal* 21, no. 5 (2013): 766-773.

[17] Srinivasacharya, D., and Ch RamReddy. "Soret and Dufour effects on mixed convection in a non-Darcy porous medium saturated with micropolar fluid." *Nonlinear Analysis: Modelling and Control* 16, no. 1 (2011): 100-115. https://doi.org/10.15388/NA.16.1.14118

[18] Mahdy, A. "Soret and Dufour effect on double diffusion mixed convection from a vertical surface in a porous medium saturated with a non-Newtonian fluid." *Journal of Non-Newtonian Fluid Mechanics* 165, no. 11-12 (2010): 568-575. https://doi.org/10.1016/j.jnnfm.2010.02.013

[19] Hayat, T., and M. Nawaz. "Soret and Dufour effects on the mixed convection flow of a second grade fluid subject to Hall and ion-slip currents." *International Journal for Numerical Methods in Fluids* 67, no. 9 (2011): 1073-1099. https://doi.org/10.1002/fld.2405
[20] Rani, Hari Ponnamma, and Chang Nyung Kim. "A numerical study of the Dufour and Soret effects on unsteady natural convection flow past an isothermal vertical cylinder." *Korean Journal of Chemical Engineering* 26 (2009): 946-954. https://doi.org/10.1007/s11814-009-0158-y
[21] Pal, Dulal, and Hiranmoy Mondal. "Effects of Soret Dufour, chemical reaction and thermal radiation on MHD non-Darcy unsteady mixed convective heat and mass transfer over a stretching sheet." *Communications in Nonlinear Science and Numerical Simulation* 16, no. 4 (2011): 1942-1958. https://doi.org/10.1016/j.cnsns.2010.08.033
[22] Sharma, Bhupendra K., Kailash Yadav, Nidhish K. Mishra, and R. C. Chaudhary. "Soret and Dufour Effects on Unsteady MHD Mixed Convection Flow past a Radiative Vertical Porous Plate Embedded in a Porous Medium with Chemical Reaction." *Applied Mathematics* 3, no. 7 (2012): 717-723. https://doi.org/10.4236/am.2012.37105
[23] Bestman, A. R. "Natural convection boundary layer with suction and mass transfer in a porous medium." *International Journal of Energy Research* 14, no. 4 (1990): 389-396. https://doi.org/10.1002/er.4440140403
[24] Awad, Faiz G., Sandile Motsa, and Melusi Khumalo. "Heat and mass transfer in unsteady rotating fluid flow with binary chemical reaction and activation energy." *PloS One* 9, no. 9 (2014): e107622. https://doi.org/10.1371/journal.pone.0107622
[25] Dhlamini, Mlamuli, Peri K. Kameswaran, Precious Sibanda, Sandile Motsa, and Hiranmoy Mondal. "Activation energy and binary chemical reaction effects in mixed convective nanofluid flow with convective boundary conditions." *Journal of Computational Design and Engineering* 6, no. 2 (2019): 149-158. https://doi.org/10.1016/j.jcde.2018.07.002
[26] Anuradha, S., and K. Sasikala. "MHD free convective flow of a nanofluid over a permeable shrinking sheet with binary chemical reaction and activation energy." *International Journal of Engineering Science Invention* 7, no. 1 (2018): 22-30.
[27] Hamid, Aamir, and Masood Khan. "Impacts of binary chemical reaction with activation energy on unsteady flow of magneto-Williamson nanofluid." *Journal of Molecular Liquids* 262 (2018): 435-442. https://doi.org/10.1016/j.molliq.2018.04.095
[28] Huang, Chuo-Jeng. "Arrhenius Activation Energy Effect on Free Convection About a Permeable Horizontal Cylinder in Porous Media." *Transport in Porous Media* 128, no. 2 (2019): 723-740. https://doi.org/10.1007/s11242-019-01267-1
[29] Mustafa, M., Junaid Ahmad Khan, T. Hayat, and A. Alsaedi. "Buoyancy effects on the MHD nanofluid flow past a vertical surface with chemical reaction and activation energy." *International Journal of Heat and Mass Transfer* 108 (2017): 1340-1346. https://doi.org/10.1016/j.ijheatmasstransfer.2017.01.029
[30] Zaib, Aurang, Mohammad Mehdi Rashidi, Ali J. Chamkha, and Krishnendu Bhattacharyya. "Numerical solution of second law analysis for MHD Casson nanofluid past a wedge with activation energy and binary chemical reaction." *International Journal of Numerical Methods for Heat & Fluid Flow* 27, no. 12 (2017): 2816-2834. https://doi.org/10.1108/HFF-02-2017-0063
[31] Monica, M., J. Sucharitha, and C. H. Kishore. "Effects of exothermic chemical reaction with Arrhenius activation energy, non-uniform heat source/sink on MHD stagnation point flow of a Casson fluid over a nonlinear stretching sheet with variable fluid properties and slip conditions." *Journal of the Nigerian Mathematical Society* 36, no. 1 (2017): 163-190.
[32] Hayat, Tasawar, Ikram Ullah, Muhammad Waqas, and Ahmed Alsaedi. "Attributes of activation energy and exponential based heat source in flow of Carreau fluid with cross-diffusion effects." *Journal of Non-Equilibrium Thermodynamics* 44, no. 2 (2019): 203-213. https://doi.org/10.1515/jnet-2018-0049
[33] Bouslimi, Jamal, M. Omri, R. A. Mohamed, K. H. Mahmoud, S. M. Abo-Dahab, and M. S. Soliman. "MHD Williamson nanofluid flow over a stretching sheet through a porous medium under effects of joule heating, nonlinear thermal radiation, heat generation/absorption, and chemical reaction." *Advances in Mathematical Physics* 2021 (2021). https://doi.org/10.1155/2021/9950993